Available online at www.sciencedirect.com
SCIENCE DIRECT®
Journal of Chromatography A, 987 (2003) 197–204
JOURNAL OF CHROMATOGRAPHY A
www.elsevier.com/locate/chroma

Microchannel-assisted thermal-lens spectrometry for microchip analysis

Eiichiro Tamaki[a], Akihide Hibara[a], Manabu Tokeshi[b], Takehiko Kitamori[a,b,c,*]

[a]*Department of Applied Chemistry, School of Engineering, University of Tokyo, 7-3-1 Hongo, Bunkyo-ku, Tokyo 113-8656, Japan*
[b]*Integrated Chemistry Project, Kanagawa Academy of Science and Technology, 3-2-1 Sakado, Takatsu-ku, Kawasaki-shi, Kanagawa 213-0012, Japan*
[c]*Precursory Research for Embryonic Science and Technology, Japan Science and Technology Corporation, Kawaguchi, Saitama 332-0012, Japan*

Abstract

Microchannel-assisted thermal lens spectrometry (MATLS) was developed for microchip analysis. This method utilized a photothermal effect in a very small space and rapid thermal conduction between a solid–liquid interface to produce a temperature gradient in the microchannel. In order to examine the mechanism experimentally, we constructed a detection system of laser defocus setup in which an excitation beam was not tightly focused, but it irradiated the microchannel homogeneously. The signal intensity dependence on modulation frequency of excitation and on solvent was investigated with the laser defocusing setup. The results of this investigation indicated that the mechanism of MATLS worked as expected. Since the mechanism of MATLS does not require directivity and coherence of the laser beam, other incoherent light sources can be used as excitation light for sensitive detections. Finally, we considered some future applications utilizing the mechanism.

Keywords: Thermal lens spectrometry; Chip technology; Instrumentation

1. Introduction

Integration of chemical processes onto microchips known as micro total analysis systems (μ-TAS) [1] or Lab-on-a-Chip [2] is receiving the attention of analytical chemists. Since microchannels of the order 10–100 μm are fabricated on the microchips and the detection volume in the microchip is very small, highly sensitive detection methods are required. Laser-induced fluorescence (LIF) and electrochemical methods have been developed to meet the sensitivity requirements. However, LIF can detect only fluorescent substances and electrochemical methods can detect only electrochemically active substances. In order to realize wider applicability, a detection method based on optical absorption is preferable. Photothermal spectrometry has sufficiently wide applicability, like light absorption methods, because it is based on non-radiative relaxation of photo-excited species. Furthermore, photothermal spectrometry has higher sensitivity than absorption methods in principle. From among photothermal spectrometry techniques, thermal lens spectrometry (TLS) is appropriate for microspace analysis [3–5]

As an important application of TLS, we have developed a thermal lens microscope (TLM). In TLM, two laser beams are coaxially introduced into

*Corresponding author. Fax: +81-3-5841-6039.
E-mail address: kitamori@icl.t.u-tokyo.ac.jp (T. Kitamori).

0021-9673/02/$ – see front matter
PII: S0021-9673(02)01661-8

a microscope. Since the objective lens has specific chromatic aberration, it is difficult to control the distance between focal points of excitation and probe beams. To overcome this difficulty, lens pairs are used to control the focus position and to adjust the distance between the two focal points. Since the distance between the two focal points can be optimized, our TLM can be applied to sensitive detection by using any kind of laser and an objective lens. Since TLM can focus the laser beam tightly by using the objective lens, it has higher spatial resolution than conventional TLS [6–8]. Furthermore, the detection point of TLM can be controlled by observing microscope images. These features of TLM make it suitable for microscale analysis such as in microchip chemistry and we have demonstrated its effectiveness as a detection method [9–12].

Although TLM has many advantages, it is very difficult to scan the excitation laser wavelength in presently available systems because a certain emission line of the laser is usually used as the excitation beam. One possibility to get wavelength scanning is to use a dye laser or other tunable laser. However, the strict optical alignment required in the dual beam configuration of TLM cannot be assured with the wavelength scanning operation of a dye laser. As long as the present principle and optical configuration are used, excitation wavelength scanning is almost impossible.

In this paper, we developed a novel TLS detection method for microchip analysis utilizing heat generation in a microchannel, where the light source of the excitation beam was not limited to a laser and strict optical alignment was not required. Our idea was based on the simple fact that a temperature distribution, which corresponds to a refractive index distribution, is important for generating the thermal lens. Conventionally, the temperature distribution is generated by utilizing the Gaussian intensity distribution of laser light and thermal diffusion around the laser beam waist. Our method is based on the mechanism of microchannel-assisted thermal lens spectrometry (MATLS). In this mechanism, the temperature distribution is generated by a heat source distribution and thermal conduction through a solid/liquid interface. In order to examine the mechanism, the temperature distribution in the microchannel under homogeneous light irradiation condition was simulated first. Then, the MATLS signal was obtained by a laser defocus thermal lens system. The simulation and experimental results showed us the mechanism of MATLS worked as expected.

2. Principle

2.1. Conventional thermal lens spectrometry

When a liquid sample is measured by TLS, changes of optothermal parameters due to thermal energy are derived from non-radiative relaxation of solute following light absorption. In TLM, the excitation and probe beams are coaxially introduced into a microscope. The excitation laser can be focused into a small spot size by the objective lens. The spot size w is expressed by:

$$w = \frac{1.22\lambda}{\text{N.A.}} \quad (1)$$

The parameters of λ and N.A. are wavelength of the laser and numerical aperture of the objective lens, respectively. For example, the excitation beam having a wavelength of 488 nm is focused into a 2.4-μm-sized spot with an objective lens having N.A. of 0.25. Spatial distribution of the light intensity is approximately the same as that of the original laser beam having a Gaussian distribution. When the sample absorbs the excitation light, a high temperature gradient is formed around the spot. Since the temperature coefficient of the refractive index is negative for an ordinary liquid, the temperature gradient acts as a concave lens, which is called the thermal lens. The thermal lens can be detected by measuring the divergence of probe beam, which is coaxial to the excitation beam. The sensitivity of TLM is 100 to 1000 times higher than that of absorption methods in principle.

2.2. Microchannel-assisted thermal lens spectrometry

In conventional TLS, the high temperature gradient to form the thermal lens is generated by utilizing the spatial distribution of laser intensity and rapid thermal diffusion in the microspace (Fig. 1a). However, the light intensity distribution is not neces-

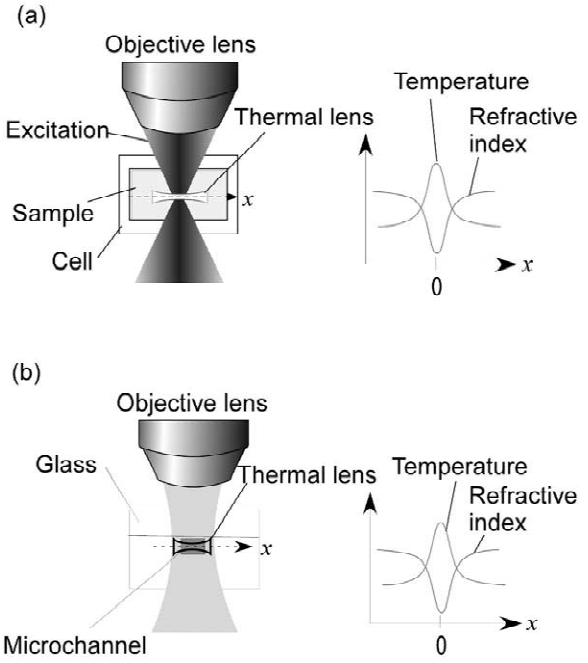

Fig. 1. Illustrations of the principle of the thermal lens effect (a) in the conventional setup and (b) in MATLS.

sary because the thermal lens can be formed by just having a sufficient temperature gradient. When thermal energy is generated in a microspace and rapidly conducted to a marginal area, a sufficiently high temperature gradient can be formed in the sample solution.

In order to generate the high temperature gradient, we propose a new mechanism utilizing a microchannel in a glass microchip. Since thermal diffusion in glass is more rapid than that in a solution in the microchannel, the temperature of the solution at the solid–liquid interface is lower than that at the center of the microchannel even under homogeneous light irradiation. If the microchannel is sufficiently narrow, the necessary high temperature gradient can be formed in the microchannel. The temperature gradient acts as the thermal lens (Fig. 1b).

3. Experimental

An Ar ion laser (wavelength, 488 nm) and a He–Ne laser (wavelength, 633 nm) were used as excitation and probe lasers, respectively. The excitation laser beam was modulated with an optical chopper and passed through a lens pair to adjust the divergence by controlling the distance between the two lenses. The focal point after the objective lens could be adjusted by changing the divergence. The two beams were coaxially aligned with a dichroic mirror and introduced into a microscope. Magnification and numerical aperture of the objective lens were ×10 and 0.25, respectively. After passing through the sample in the microchannel, the excitation laser was cut by a high-pass-filter. The probe beam was condensed and measured with a photodiode. As the probe light was being measured by the photodiode, it was synchronously detected with a lock-in-amplifier. The glass microchip consisted of upper-, middle- and lower-plates (170, 100 and 500 μm in thickness, respectively) [9]. The microchannel was fabricated in the 100-μm-thick middle-plate by a CO_2 laser and had a width of 250 μm. The three plates were thermally bonded without any adhesive. The sample was introduced into the microchannel with a syringe pump through a capillary [9]. The conditions of the setup are summarized in Table 1.

4. Results and discussion

4.1. Simulation

In order to confirm the idea of MALTS, the temperature distribution in the microchannel under

Table 1
Parameters of experimental setup

Excitation laser	Ar ion laser (488 nm)
Probe laser	He–Ne laser (633 nm)
Objective lens	×10 (magnification) 0.25 (N.A.)
Dimension of the microchannel	250 μm (width)×100 μm (depth)

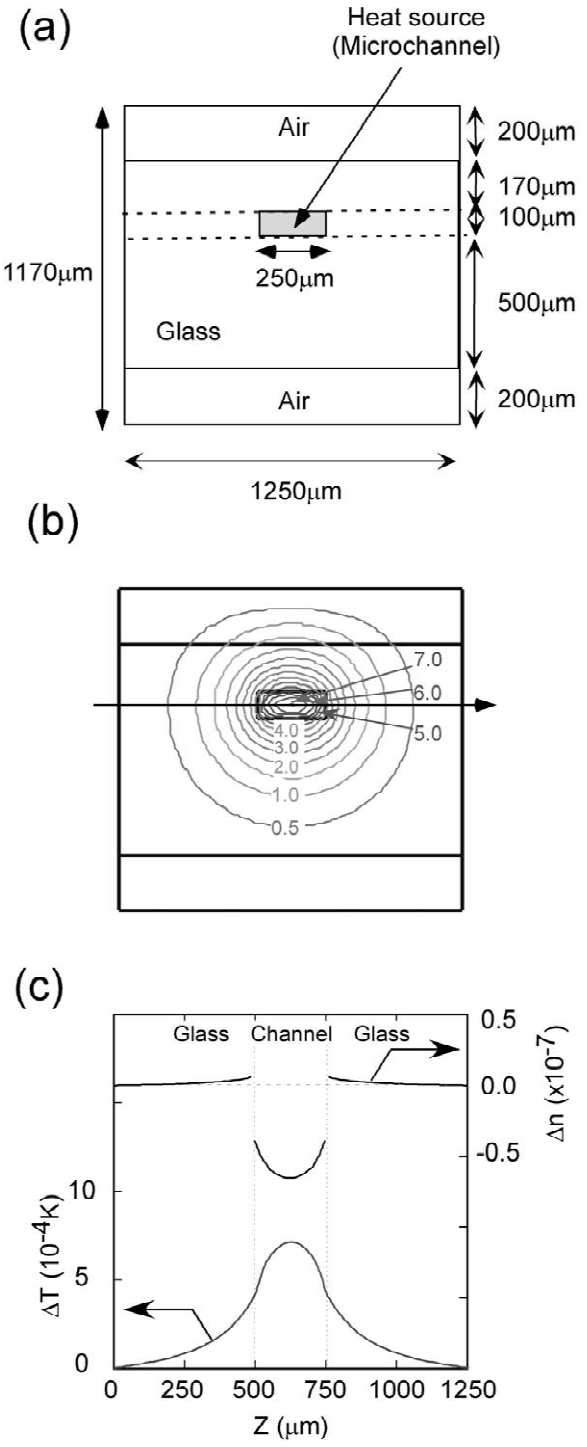

Fig. 2. (a) Illustration of the simulated area. The whole calculated area is 1250 μm ×1170 μm and the microchannel has 250-μm width and 100-μm depth. (b) Simulation results after 0.1 s. The heat is homogeneously generated in the microchannel with a rate of 0.1 mW/mm^3. The numbers in the figure express temperature change (unit of the numbers is 10^{-4} K). (c) One-dimensional temperature and refractive index distributions along the arrow in Fig. 2(b).

homogeneous light irradiation was simulated numerically by a two-dimensional finite element method. Fig. 2a shows a cross-sectional view of the simulated area, 1250 μm wide and 1170 μm high. The simulation area consisted of air, the glass substrate of the microchip and the liquid in the microchannel. Air layers (200-μm-thick) were present on both top and bottom sides of the 770-μm-thick glass substrate layer. The microchannel, 250 μm wide and 100 μm deep, was located 170 μm from the top edge of the glass. We confirmed the 200-μm-thick air is sufficient thickness for this simulation by simulating the other condition (data not shown). At the boundary of the simulation area, temperature change was assumed to be zero. The heat source term was assumed to be homogeneous in the liquid phase in the microchannel and to turn on and off at an interval of 0.1 s. An aqueous solution of dye was assumed as a typical sample. The physical parameters are summarized in Table 2. The physical parameters of water, air and methanol were taken from the textbook by Bialkowski [13]. Physical parameters of fused-silica depend on the preparation method. Therefore, typical values were used. The temperature coefficient of refractive index was cited from a handbook [14]. Other parameters of fused-silica were provided by the glass manufacturing company.

Under the above conditions, we numerically solved the thermal diffusion equation with the two-dimensional finite element method. The thermal diffusion equation is expressed by:

$$\frac{\partial}{\partial t}\delta T(x,y,t) - D_T \nabla^2 \delta T(x,y,t) = \frac{Q_H(x,y)}{\rho C_P} \qquad (2)$$

The parameters of D_T, Q_H, ρ and C_P are thermal diffusion constant of solvent, heat generation rate, density of solvent, and heat capacity of solvent, respectively. These parameters, except for Q_H are

Table 2
Physical parameters used in the calculation

	Thermal conductivity ($W\ m^{-1}\ K^{-1}$)	Heat capacity ($J\ kg^{-1}\ K^{-1}$)	Density ($kg\ m^{-3}$)	$\frac{dn}{dT}$ (K^{-1})
Water [13]	0.598	$4.18\cdot10^{3}$	$1.0\cdot10^{3}$	$-9.1\cdot10^{-5}$
Glass [14] (fused-silica)	1.4	$0.67\cdot10^{3}$	$2.2\cdot10^{3}$	$1.2\cdot10^{-5}$
Air [13]	$2.61\cdot10^{-2}$	$1.01\cdot10^{3}$	1.17	$-0.88\cdot10^{-6}$
Methanol [13]	0.202	$2.46\cdot10^{3}$	$0.79\cdot10^{3}$	$-3.49\cdot10^{-4}$

given in Table 2. Q_H is zero in glass and air solvent and 0.1 mW/mm^3 in aqueous solvent. For example, a concentration of 10^{-7} *M*, an absorption coefficient per molar of 10^4 $cm^{-1}\ M^{-1}$ and laser power of 10 mW are necessary for this heat generation. The simulation results after 0.1 s for a heat generation rate of 0.1 mW/mm^3 are shown in Fig. 2b as temperature contours. The one-dimensional temperature and refractive index distributions along the arrow in Fig. 2b are shown in Fig. 2c. According to the refractive index distribution in the microchannel, the focal length of the thermal lens was estimated to be $-1.24\cdot10^4$ m, which is sufficient for detection. Fig. 3 shows the time course of temperature at the center of the microchannel when the heat generation was switched at a frequency of 5 Hz. The temperature changes at the center of the microchannel represented the thermal lens effect and the time course showed that the deformation of the thermal lens effect as well as the formation were similar to those in conventional TLS.

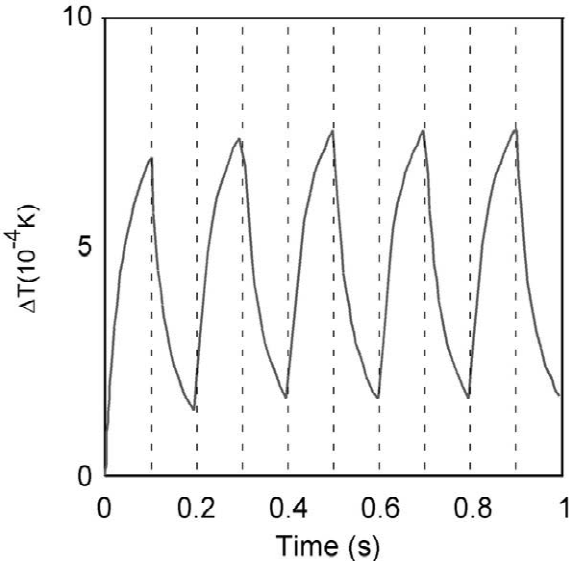

Fig. 3. Time course of the simulated temperature at the center of the microchannel with intermittent excitation at the frequency of 5 Hz.

4.2. Modulation frequency mechanism of MATLS

In order to verify the mechanism of MATLS, a modified TLM setup called the laser defocusing setup was constructed. In this setup, the excitation laser was broadly irradiated onto the microchannel. In conventional TLM, the excitation beam is focused onto the liquid in the microchannel. In the laser defocusing setup, the focus of the excitation beam was positioned at 500 μm under the microchannel and the probe beam was focused in the upper part of the microchannel. Illustrations of this setup and the conventional one are shown in Fig. 4.

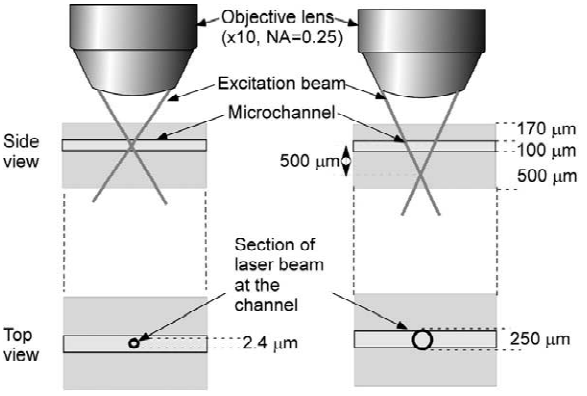

Fig. 4. Illustrations of optical setup at the microchannel under the objective lens for (a) the conventional and (b) laser defocusing setups. Photographs of the excitation beam with these setups are also shown.

Firstly, modulation frequency dependences of the thermal lens signals with the laser defocusing and conventional setups were compared in order to discuss the signal propagation processes. The reciprocal of modulation frequency was approximately equivalent to the excitation light irradiation time in each process of signal forming. Therefore, the signal propagation process could be inspected by changing the modulation frequency. The thermal lens signal of 10^{-4} *M* aqueous solution of Sunset Yellow dye was measured at various modulation frequencies in the conventional and laser defocusing setups.

The modulation frequency dependences of the signal intensity are shown in Fig. 5a. In the high modulation frequency region around 1 kHz, the signal intensity with the conventional setup had a higher intensity than with the laser defocusing setup. The difference could be explained by the difference in the principle of the thermal lens formation. In the conventional setup, thermal diffusion around the excitation beam spot was the dominant process for the formation. Thermal diffusion time required for a 10-μm-sized space was estimated as being of the order of 1 ms. On the other hand, the thermal lens signal in the laser defocusing setup rapidly decreased while increasing the modulation frequency because thermal conduction between the glass–liquid interface was the dominant process for the thermal lens formation. In the laser defocusing setup, thermal diffusion length was of the order of 100 μm, where 100 ms were required as diffusion time. By contrast, in the low frequency region, the signal intensity of both the laser defocusing and conventional setups had a similar tendency. This observation meant that the microchannel-assisted thermal lens mechanism worked even in the conventional setup at low frequency. We must note that the gaussian intensity profile itself can contribute to the signal in laser defocusing setup experiment because using laser. We confirmed that its contribution to the signal is not of major significance by another simulation (data not shown).

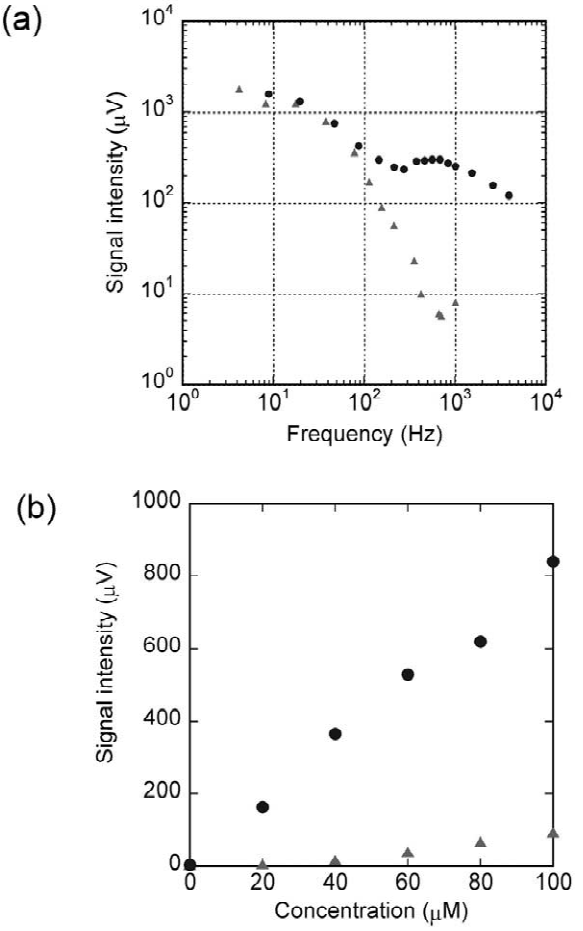

Fig. 5. (a) Modulation frequency dependence of the signal in the conventional (circles) and laser defocusing (triangles) setup. (b) Concentration dependence of the methanol (circles) and aqueous (triangles) solution signals for Sunset yellow dye.

4.3. MATLS signal dependence on solvent

Next, for further confirmation of the signal origin, we measured solvent dependence of the MALTS signal. Generally, the thermal lens signal depends on thermal and optothermal parameters of the solvent. The enhancement factor *E* of the thermal lens signal in the conventional TLS is defined as:

$$E = \frac{P\left(\frac{dn}{dT}\right)}{\lambda\kappa} \quad (3)$$

where *P*, λ and κ are laser power, wavelength of the probe beam and thermal conductivity of solvent, respectively. In order to compare the enhancement of the MATLS signal, water and methanol were chosen as solvents. According to Eq. (2) and the parameters shown in Table 2, methanol has a 12.9-times-higher

enhancement than water in conventional TLS. Calibration curves of MATLS signals of aqueous and methanol solutions of Sunset Yellow dye are shown in Fig. 5b. Modulation frequency was 70 Hz. The linearity of the thermal lens signal to dye concentration in both solvents was confirmed. Comparing the gradients of both calibration curves showed the signal of the methanol solution had 8.5 times higher sensitivity than that of the aqueous solution. Although the enhancement factor of MATLS cannot be directly compared with that of TLS due to the difference in principle, the 8.5 times enhancement of methanol to water could be considered to indicate that the MATLS signal originated in photothermal phenomena.

4.4. Limits of detection

The calculated LODs (limit of detection) of MATLS with the Ar ion laser was $2 \cdot 10^{-5}$ Abs. The laser light intensity at the sample was 42 mW. It seems that an LOD of the order of 10^{-4} Abs of LOD is required for microchip analysis. According to the results, the required LOD can be obtained with several milliwatt light intensity. Even if the white light is monochromated, this light intensity is secured.

4.5. Advantages of MATLS

According to these simulation and experimental results, we concluded that the mechanism of MATLS worked as we expected. Although a laser was used as the light source, directivity and coherence of the laser are not always required for the excitation laser source with MATLS. This means that various light sources, including an incoherent tunable source, can be applied to thermal lens detection. Another advantage of MATLS is the ease of optical alignment. While a strict optical alignment of the sub-μm order is required for conventional TLM, MATLS needs just a simple optical setup. This feature allows the conditions of the light source to be changed and it is appropriate for tuning the excitation wavelength.

Chartiar and Bialkowski [15] measured the thermal lens signal by irradiating a wide bandwidth white light onto a metal cylindrical cell, based on a similar principle to MATLS. However, since their cell was larger and the modulation frequency was 100 mHz, it would be difficult to be directly applied to flow analysis in the microchannel. As to the sample cell size and modulation frequency, we detected the thermal lens signal in the 250-μm-sized microchannel with the modulation frequency of the order of 70 Hz, which is more appropriate to detect flowing liquid in the microchannel.

In this method, we can apply any light source, we are not limited to lasers, for microchip flow analysis.

5. Conclusion

We developed a novel detection method for microchip flow analysis by using TLS. We verified the mechanism of MATLS method both by simulation and experiments. By this method, various kinds of light can be used for excitation and we will develop wavelength-tunable thermal lens microscopy in the future. The future wavelength tunable microscopy system will be a powerful detection tool for chromatography or capillary electrophoresis.

Acknowledgements

This research was partially supported by Asahi Kasei Corporation, Shimadzu Science Foundation and by the Ministry of Education, Science, Sports, Culture and Technology of Japan, Grant-in-Aid for Encouragement of Young Scientists, 12750712, 2000, and Grant-in-Aid for Scientific Research for University and Social Collaboration, 11974006, 1999.

References

[1] D.J. Harrison, A. van den Berg (Eds.), Micro Total Analysis Systems ‘98, Kluwer, Dordrecht, 1998.
[2] M. Freemantle, Chem. Eng. News (1999) Feb. 22, 27.
[3] K.J. Skogerboe, E.S. Yeung, Anal. Chem. 58 (1986) 215.
[4] Z. Rosenweig, E.S. Yeung, Appl. Spectrosc. 47 (1993) 1175.
[5] W.A. Weimer, N.J. Dovichi, Anal. Chem. 60 (1988) 662.
[6] M. Tokeshi, M. Uchida, K. Uchiyama, T. Sawada, T. Kitamori, J. Lumin. 83–84 (1999) 261.
[7] K. Uchiyama, A. Hibara, H. Kimura, T. Sawara, T. Kitamori, Jpn. J. Appl. Phys. 39 (2000) 5316.

[8] M. Tokeshi, M. Uchida, A. Hibara, T. Sawada, T. Kitamori, Anal. Chem. 73 (2001) 2112.
[9] M. Tokeshi, T. Minagawa, T. Kitamori, Anal. Chem. 72 (2000) 1711.
[10] K. Sato, M. Tokeshi, H. Kimura, T. Kitamori, Anal. Chem. 73 (2001) 1213.
[11] M. Tokeshi, T. Minagawa, K. Uchiyama, A. Hibara, K. Sato, H. Hisamoto, T. Kitamori, Anal. Chem. 74 (2002) 1565.
[12] E. Tamaki, K. Sato, M. Tokeshi, K. Sato, M. Aihara, T. Kitamori, Anal. Chem. 74 (2002) 1560.
[13] S.E. Bialkowski, Photothermal Spectroscopy Methods for Chemical Analysis, in: Wiley, New York, 1996, p. 425.
[14] American Institute of Physics Handbook, in: 3rd ed., McGraw Hill, New York, 1973, p. 6.
[15] A. Chartiar, S.E. Bialkowski, Opt. Eng. 36 (1997) 303.